

Solid state sintering of very low and negative thermal expansion ceramics by Spark Plasma Sintering

Olga García-Moreno^{a,*}, Adolfo Fernández^b, Ramón Torrecillas^a

^a Centro de Investigación en Nanomateriales y Nanotecnología, CINN (Consejo Superior de Investigaciones Científicas – Universidad de Oviedo – Principado de Asturias), Parque Tecnológico de Asturias, 33428 Llanera, Spain

^b Fundación ITMA, Parque Tecnológico de Asturias, 33428 Llanera (Asturias), Spain

Received 22 September 2010; received in revised form 29 October 2010; accepted 17 November 2010

Available online 25 December 2010

Abstract

Lithium aluminosilicate powder precursors of compositions $\text{Li}_2\text{O}:\text{Al}_2\text{O}_3:\text{SiO}_2$ as 1:1:2; and 1:1:3.11 were synthesized and sintered by the Spark Plasma Sintering technique. The sintering conditions were adjusted to obtain dense ceramic materials in an attempt to avoid the presence of a glassy phase. XRD and SEM images were employed for composition and microstructure characterization. The coefficient of thermal expansion of the sintered samples was studied down to cryogenic conditions. Rietveld quantification was performed with the use of an external standard. Pure β -eucryptite of different compositions in dense ceramic bodies was obtained with a negative expansion coefficient.

© 2011 Elsevier Ltd and Techna Group S.r.l. All rights reserved.

Keywords: Negative thermal expansion; Dilatometry; Lithium aluminosilicates

1. Introduction

Ultrastable materials are required in a wide range of precision devices and instrument equipment in high-tech systems in microelectronics or optical precision applications. Whenever dimensional stability is required with temperature changes for any precision element, it will be necessary to lower the coefficient of thermal expansion (CTE) of materials employed for constructing that element. This property can be achieved by two main approaches: by using materials with a very low CTE and by designing composite materials with positive and negative CTE phases that produce a null bulk CTE. The second approach is one of the main applications of negative thermal expansion materials.

Sintered negative thermal expansion materials usually have low mechanical strength because the expansion anisotropy causes microcracking. This is due to very different thermal expansions in different crystallographic orientations that induce internal stress with temperature changes. Although some negative expansion materials, such as sodium zirconium

phosphate, have improved mechanical properties [1], these properties are still insufficient for many applications in the lithium aluminosilicate system [2,3].

Among the negative thermal expansion materials family, β -eucryptite is one of the most thoroughly studied. β -Eucryptite is the most negative thermal expansion phase in the lithium aluminosilicate system (LAS) [2,3]. The widespread use of LAS glass-ceramics, from cooktops in millions of households to mirror blanks used in outer space, led to a detailed study into the lithium aluminosilicate system [4]. The negative expansion phase in the LAS system is β -eucryptite (LiAlSiO_4) while spodumene ($\text{LiAlSi}_2\text{O}_6$) has almost zero expansion.

β -Eucryptite structure is a stuffed derivative of the high-quartz structure where half of the Si^{4+} ions are replaced by Al^{3+} ions and charge balanced by Li^+ ions. The thermal expansion behavior of β -eucryptite is closely related to its structure. The bulk α value for β -eucryptite is negative for a wide temperature range even when α_a and α_b can be positive because α_c values are largely negative.

The traditionally used method for the manufacturing of LAS materials is the glass-forming technique to produce glass-ceramics. This method implies the fabrication of molten material, which is later shaped and heat treated. The ceramic products manufactured by this method are some times

* Corresponding author. Tel.: +34 985 98 00 58; fax: +34 985 26 55 74.

E-mail address: o.garcia@cinn.es (O. García-Moreno).

inhomogeneous [4]. Occasionally it is also necessary to have a ceramic body without or with very small proportions of a glassy phase which lower the rigidity and resistance of the ceramic product. Compared with the number of studies of the glass-ceramic approach there are few studies in the literature that deal with this system as a ceramic material in the solid state [2,5,6]. This is important because as far as it is possible to obtain 100% theoretical dense materials in this system in the solid state, the mechanical properties and the modulus of elasticity will be improved in relation to the glass-ceramic materials with similar thermal shock characteristics. The reason for the lack of work in solid state sintering is the narrow sintering window in the LAS system and the easy formation of melts at low temperatures that make it difficult to obtain dense material in this system. In the work presented here we will deal with ceramic materials with no or with negligible amounts of a glassy phase.

The ceramics fabrication by Spark Plasma Sintering (SPS) technique is here proposed as a solution to this problem. The SPS technique can lead to high relative densities with no or with very low amounts of a glassy phase. The ability of this sintering technique to obtain dense ceramics will be demonstrated. Previous studies have shown that even for pressureless sintering methods it is necessary to control the sinterability of these ceramics [7] and the variations of thermal expansion coefficient with the LAS composition [8].

For these purposes, two different β -eucryptite solid solution compositions were synthesized and sintered. The SPS technique will be evaluated for obtaining dense ceramic LAS bodies with high density and a very low glass proportion. It should be noted that ceramics in this system sintered by this method are very scarce in the literature [9]. Finally, the ceramic properties will be evaluated by a study of their thermal expansion behavior.

2. Experimental procedure

2.1. Materials

β -Eucryptite s.s. powders with a composition between eucryptite and spodumene were synthesized for this study following the route proposed in a previous work (see [7] for details). The chemical compositions of the LAS powders correspond to a $\text{Li}_2\text{O}:\text{Al}_2\text{O}_3:\text{SiO}_2$ relation of 1:1:2 and 1:1:3.11, named L2 and L3 respectively in this paper. The oxide composition is detailed in Table 1.

The LAS powders thus synthesized were composed of β -eucryptite s.s. Traces of quartz and spodumene were found in L3, as shown in the diffractogram of Fig. 1.

Table 1
Oxide composition of L2 and L3 eucryptite powders.

Sample	Li_2O	Al_2O_3	SiO_2	$\text{Li}_2\text{O}:\text{Al}_2\text{O}_3:\text{SiO}_2$
L3	9.0	31.0	60.0	1:1:3.11
L2	11.9	40.5	47.7	1:1:2

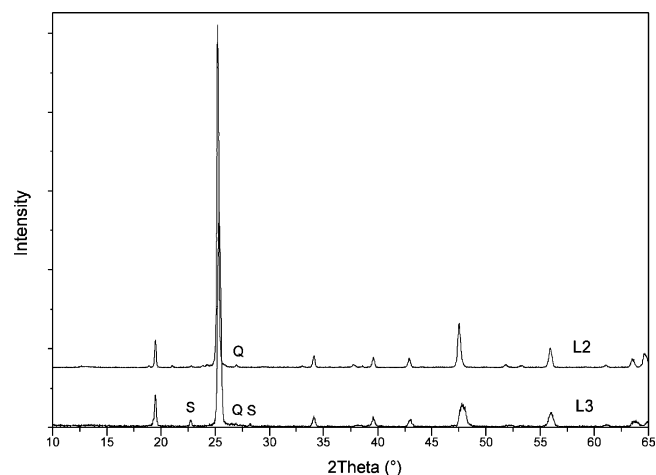


Fig. 1. Diffractogram of the starting material powders L2 and L3. The diffraction maxima correspond to β -eucryptite phase (PDF file #870602 and 251183), traces of quartz and spodumene are marked by Q and S respectively.

2.2. Sintering and characterization

The powders were uniaxially pressed in 20 mm diameter graphite dies for Spark Plasma Sintering experiments. A Spark Plasma apparatus HPD25/1 from FCT was used. The SPS apparatus generated electrical power, which was delivered through the die in rapid pulses. A vacuum was maintained in the apparatus during the sintering process. The external force applied to the die was either 5 or 20 kN (16 or 65 MPa respectively). The samples were fired at a heating rate of 100 K/min to temperatures between 1100 and 1300 °C with a short dwell time of 2 min, and free cooling.

Surfaces of sintered specimens were prepared for scanning electron microscopy (SEM Zeiss DSM 950) by diamond polishing to 1 μm . Polished surfaces were also observed by SEM and by Field Emission-Scanning Electron Microscopy (FE-SEM (Zeiss Ultraplus)). Bulk densities and apparent porosities were measured by the Archimedes method using deionized water as the immersion medium.

X-ray diffraction (XRD) analysis was used to identify the phases present in the powdered and sintered materials. XRD patterns were obtained using a diffractometer (Model D5000, Siemens, Karlsruhe, Germany) with $\text{CuK}\alpha$ radiation operated at 40 kV and 30 mA ($\lambda = 0.15418 \text{ nm}$). Patterns were recorded over the goniometer range of 10–65° with a step size of 0.02° and a counting time of 1 s per step. The levels of the β -eucryptite and glass phases in the ceramic materials were determined by XRD Rietveld phase composition analysis. Rietveld refinement calculations were conducted with a MAUD program [10]. Absolute levels of the glass phase for the β -eucryptite ceramics were derived using a Rietveld procedure, with Aldrich 99.99% CaF_2 as external standard material. The crystal structure models used for the β -eucryptite were those corresponding to ICDS codes 24896 and 24988; and 82707 for fluorite. Traces of spodumene (55665 ICDS) were identified in some L3 sintered samples. The glassy phase content was determined indirectly by the difference between the sum of phase levels and 100%.

Table 2

Density and CTE values of the sintered L2 and L3 samples.

Sample	Temperature (°C)	Force (kN)	Density (g/cm ³)	CTE –150 to +150 °C (K ^{−1})	CTE –150 to +450 °C (K ^{−1})
L2	1100	5	99.2	-0.6×10^{-6}	1.1×10^{-6}
	1100	20	99.2	-0.7×10^{-6}	1.3×10^{-6}
	1200	5	99.1	-0.6×10^{-6}	1.2×10^{-6}
	1200	20	99.0	-0.4×10^{-6}	1.4×10^{-6}
	1300	5	100.0	-0.7×10^{-6}	1.0×10^{-6}
L3	1100	5	99.4	-1.8×10^{-6}	-0.7×10^{-6}
	1100	20	99.7	-1.6×10^{-6}	-0.6×10^{-6}
	1200	5	98.8	-1.9×10^{-6}	-0.9×10^{-6}

The coefficient of thermal expansion was checked in a Netzsch DIL402C between −150 and 450 °C.

3. Results and discussion

3.1. Sintering by SPS: density and composition

Table 2 summarizes the results in terms of density and CTE of the SPS samples. Both using L2 and L3 starting powder materials; β -eucryptite was identified, by XRD, to be the major phase present in all cases. Density values were very high and close to theoretical values for both compositions L2 and L3. Even for relatively low temperature (1100 °C) density increased remarkably in comparison with density values obtained by means of pressureless conventional sintering [7,11].

Fig. 2 shows the shrinkage during sintering in terms of speed of piston die displacement versus temperature, for the highest temperature sintered samples by SPS. Sintering of L3 sample started at lower temperature (around 750°) reaching a maximum speed displacement at approximately 900 °C. L2 sample started sintering at a higher temperature of 850 °C, with a maximum speed displacement of around 1000 °C. Both samples seemed to finish sintering at similar temperature 1100–1150 °C.

3.2. Coefficient of thermal expansion

The coefficient of thermal expansion was very low for all the samples, with values between -1.9 and $+1.3 \times 10^{-6}$, depend-

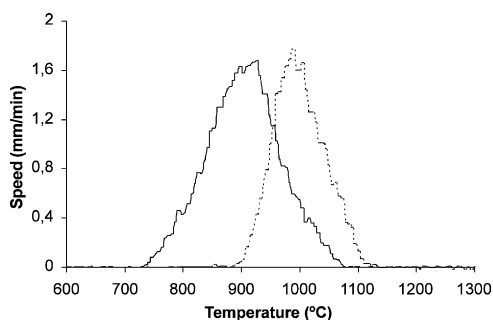


Fig. 2. Speed of piston die displacement for L2 (discontinuous line) and L3 (continuous line) samples in SPS. The final temperature of the treatment was 1300 °C for L2 and 1200 °C for L3; heating rate: 100 °C min^{−1} and 5 kN force.

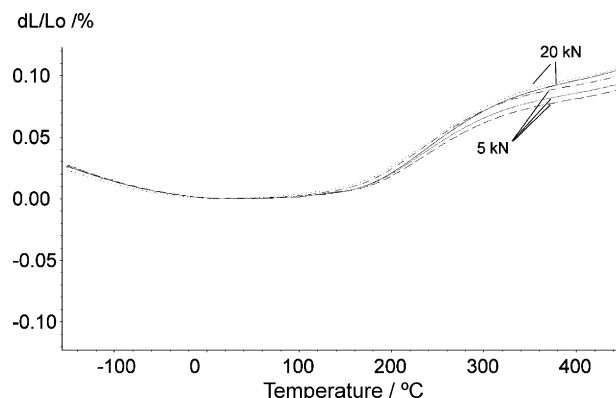


Fig. 3. Thermal expansion (dL/Lo (%)) with temperature for the L2 sintered samples at 20 kN in grey (1100 °C, continuous line; and 1200 °C, dotted line) and 5 kN in black (1100 °C, continuous line; 1200 °C, discontinuous and dotted line; and 1300 °C, discontinuous line).

ing on the sample composition and the temperature interval of the measurement. In general, as can be seen in Figs. 3 and 4, the sintered LAS samples have negative expansion behavior in the low temperature range, which changed to positive in the high temperature range. This change in the slope of the elongation curve was stronger for the L2 sintered samples (Fig. 3) and smoother in the case of L3 samples. In L3 samples, a roughly flat curve can be observed between +100 and +300 °C, with almost null elongation (Fig. 4). The temperature interval in which L2 samples show the lowest elongation was slightly lower than in L3 samples: from room temperature to +150 °C.

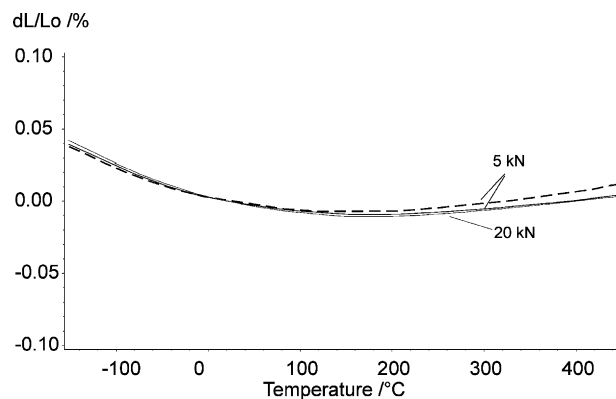


Fig. 4. Thermal expansion (dL/Lo (%)) with temperature for the L3 sintered samples at 1100 °C/5 kN (grey continuous line), 1100 °C/20 kN (black continuous line) and 1200 °C/5 kN (black discontinuous line).

From this to higher temperatures, the slope changed again sharply to +300 °C, and again became smoother to +450 °C. This change in the slope and sign of the CTE value with increasing temperature has been observed in similar compositions in other studies of low expansion ceramics [12].

The variations of the elongation and CTE behavior of each composition for different sintering temperature and pressure conditions were very small. For L2 composition, it seems that the elongation values were higher when the samples were sintered under higher pressure as can be seen in Fig. 3. The variations with the sintering temperature were even smaller and negligible in the low temperature range of the measurements.

3.3. X-ray diffraction of the sintered samples. Phase quantification

Structural characterization of the sintered samples by XRD showed stability of the β -eucryptite phase with temperature during sintering. No other phases were identified, and traces of quartz and spodumene present in the starting powder material seemed to react out. It is noticeable that β -eucryptite was stable without any need for additives like Zr_2O [12] for the studied temperature range and for both compositions. The L3 sintered sample gave a more silica-rich β -eucryptite solid solution phase with space group P6222 (ICSD-24896, Al_{1.32} Li_{1.146} O₆ Si_{1.68} [13]) than the L2 sintered samples (ICSD-24888, Al₁ Li₁ O₄ Si₁ [14]), with β -eucryptite superstructure, with space group P6422. This is in agreement with the composition of the starting material (Table 1). Rietveld refinement and quantification was performed for the sintered samples described in Table 3. Some LAS powders with compositions L2 and L3 were also calcined in a conventional furnace, and quantification of a glass phase in these powders is also shown in Table 3. The estimated glass proportions in all cases for the sintered samples were below 2 wt.%. This was also the case for the L2 samples calcined up to 1300 °C. L3 calcined samples exhibited a higher glass amount, around 5 wt.% for 1300 °C. This is in agreement with the SPS experiments performed with L3 powders. At 1300 °C the vitreous phase formed during sintering was high enough to extrude from the graphite die and it was impossible to obtain a dense ceramic disk at this temperature, and data concerning this sample are not included in the tables. Nevertheless, L3 samples sintered at 1200 °C (5 kN) by SPS

Table 3

Rietveld quantification of glass phase formed in L2 and L3 SPS sintered samples at different temperatures under the same force (5 kN), and L2 and L3 conventionally calcined powders.

	Sample	Temperature (°C)	Glass (wt.%)
SPS	L3	1100	<2%
		1200	<2%
	L2	1200	<2%
		1300	<2%
Conventional	L3	1100	2
		1300	5
	L2	1100	<2%
		1300	<2%

gave high density values (Table 2), and also 1100 °C with higher pressure (20 kN) gave almost theoretical density values. In conventional sintering methods [7] it was necessary to elevate the temperature up to 1300 °C to obtain only 96% density [7].

3.4. Microstructures

Fig. 5 shows SEM and FE-SEM images of polished surfaces of two L3 sintered samples. The presence of very low porosity can be observed in Fig. 5a, corresponding to a low pressure and low temperature sintered sample. The composition of the crystal and the vitreous phases was very similar. This makes it very difficult to obtain good Z-contrast images with back-scattered electrons in these samples. For details of the glassy phase, FE-SEM images were obtained. Fig. 5b shows a more detailed picture of a higher temperature sintered sample with no pores. In this picture the several micron β -eucryptite crystals can be observed surrounded by a thin layer of vitreous phase (lighter grey). This small amount of glass phase could not be quantified by XRD methods as described above, and is estimated to be below 2 vol.% by image analysis (greyscale discerned images).

Microstructure has a strong influence in the mechanical properties. The high dense LAS ceramics obtained by SPS was mechanically characterized [15]. Fracture strength values increased from 60 MPa, obtained in conventional sintered samples at 1300 °C, to 140 MPa in the SPS sintered sample at 1200 °C.

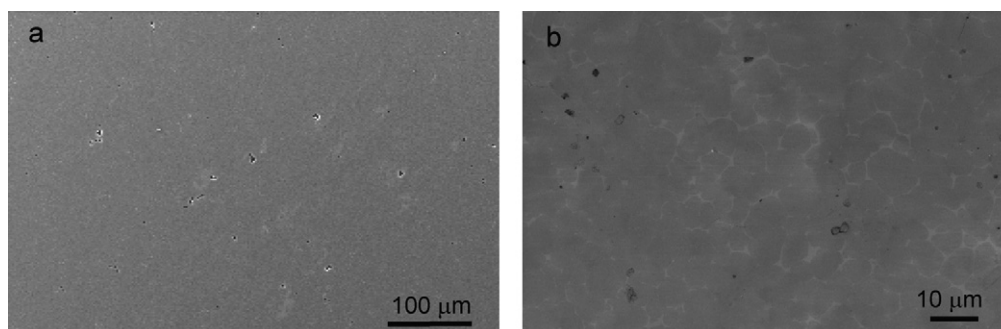


Fig. 5. SEM (a) and FE-SEM (b) images corresponding to L3 sample sintered at 1100 °C/5 kN and 1200 °C/5 kN respectively.

4. Conclusions

Almost negligible amounts of a glass phase were detected in β -eucryptite dense sintered ceramics by SPS methods at different pressures. For composition 1:1:2, negative expansion ceramics were obtained up to 1300 °C for the low temperature range of CTE measurements. The elongation changed to positive at higher temperatures. For composition 1:1:3.3, the higher sintering temperature for negligible amounts of glassy phase was 1200 °C. The elongation behavior of samples with this composition was negative in a wider temperature range of the CTE measurement. In both cases, the density values obtained by SPS were improved compared to conventional sintering methods, reaching >99.5 t.d.% values for relatively low sintering temperatures.

5. Acknowledgments

The authors greatly appreciate the support of the EU for the IP-Nanoker NMP3-CT-2005-515784 in the context of the 6th Framework Program. García-Moreno is working for CSIC under a JAE-Doc contract co-funded by the ESF.

References

- [1] P. Oikonomou, C. Dedeloudis, C.J. Stournaras, C. Ftikos, [NZP]: a new family of ceramics with low thermal expansion and tunable properties, *J. Eur. Ceram. Soc.* 27 (2–3) (2007) 1253–1258.
- [2] W.I. Abdel-Fattah, R. Abdellah, Lithia porcelains as promising breeder candidates – I. Preparation and characterization of [beta]-eucryptite and [beta]-spodumene porcelain, *Ceram. Int.* 23 (6) (1997) 463–469.
- [3] G.J. Sheu, J.C. Chen, J.Y. Shiu, C. Hu, Synthesis of negative thermal expansion TiO₂-doped LAS substrates, *Scripta Mater.* 53 (5) (2005) 577–580.
- [4] H. Bach, *Low Thermal Expansion Glass Ceramics*, Springer-Verlag, Berlin, 1995.
- [5] W.I. Abdel-Fattah, F.M. Ali, R. Abdellah, Lithia porcelains as promising breeder candidates – II. Structural changes induced by fast neutron irradiation, *Ceram. Int.* 23 (6) (1997) 471–481.
- [6] S. Mandal, S. Chakrabarti, S. Ghatak, Preparation and characterization of a powder precursor, consisting of oxides of Li–Al–Si in the form of hydroxyhydrogel for synthesis of [beta]-spodumene ceramics, *Ceram. Int.* 30 (3) (2004) 357–367.
- [7] O. García-Moreno, A. Fernández, S. Khainakov, R. Torrecillas, Negative thermal expansion of lithium aluminosilicate ceramics at cryogenic temperatures, *Scripta Mater.* 63 (2010) 170–173.
- [8] J. Smoke, Ceramic composition having negative linear thermal expansion, *J. Am. Ceram. Soc.* 34 (3) (1951) 87–90.
- [9] P. Riello, S. Bucella, L. Zamengo, U. Anselmi-Tamburini, R. Francini, S. Pietrantonio, Z.A. Munir, Erbium-doped LAS glass ceramics prepared by spark plasma sintering (SPS), *J. Eur. Ceram. Soc.* 26 (15) (2006) 3301–3306.
- [10] L. Lutterotti, Total pattern fitting for the combined size–strain–stress–texture determination in thin film diffraction, *Nuclear Instrum. Methods Phys. Res., Sect. B: Beam Interact. Mater. Atoms* 268 (3–4) (2010) 334–340.
- [11] S. Mandal, S. Chakrabarti, S. Das, S. Ghatak, Sintering characteristics of in situ formed low expansion ceramics from a powder precursor in the form of hydroxy hydrogel, *Ceram. Int.* 30 (8) (2004) 2147–2155.
- [12] S. Mandal, S. Chakrabarti, S.K. Das, S. Ghatak, Synthesis of low expansion ceramics in lithia–alumina–silica system with zirconia additive using the powder precursor in the form of hydroxyhydrogel, *Ceram. Int.* 33 (2) (2007) 123–132.
- [13] L. Chi-Tang, The crystal structure of Li₂Al₂Si₃O₁₀ (high-quartz solid solution), *Zeitschrift fuer Kristallographie, Kristallgeometrie, Kristallphysik, Kristallchemie* 132 (1970) 118–128.
- [14] V. Tscherry, H. Schulz, Synthesis and X-ray reflection pattern of beta-eucryptite, *Naturwissenschaften* 57 (1970) 194.
- [15] A. Borrell, Nuevos materiales ultrafuncionales cerámica/nanofibras de carbono, Universidad de Oviedo, PhD, 2010, 272.